IN-SITU MEASUREMENTS OF THE KINETICS OF SPINEL GROWTH ON MgO-SLAG (CaO-Al$_2$O$_3$-SiO$_2$) COUPLES

Brian J. Monaghan[1] and Sharon A. Nightingale[2]

1. Author correspondent, Senior Lecturer, PYROmetallurgical Group, Faculty of Engineering, University of Wollongong, Northfields Ave. Wollongong, NSW 2522, Australia, 61-2-42214580, monaghan@uow.edu.au.
2. Assoc Professor, PYROmetallurgical, Faculty of Engineering, University of Wollongong, Northfields Ave. Wollongong, NSW 2522, Australia, 61-2-42213775, sharon@uow.edu.au

ABSTRACT

The growth of spinel crystals on single crystal MgO in a CaO-Al$_2$O$_3$-SiO$_2$ slag has been investigated over the temperature range 1420°C to 1460°C using high temperature microscopy. Key findings of the investigation were that the spinel crystal that grew on the MgO had a well developed faceted morphology and displayed an octahedral form of a cubic crystal bounded by (111) planes. After a period of time the crystal detached from the MgO, floated off into the slag and dissolved. From kinetic analysis it was found that the spinel crystal growth rate was consistent with the parabolic rate law. Arrhenius constants were evaluated to establish the temperature dependence of the parabolic growth rate constant. The activation energy for growth of the spinel layer was found to be 564 kJmol.$^{-1}$.

INTRODUCTION

It is known that the formation of a spinel layer on MgO refractories can offer protection from slag attack in many metallurgical processes. If this process to be fully understood and characterized then a more detailed knowledge of the kinetics of layer formation process is required.

During dissolution of MgO immersed in molten slags containing Al_2O_3, various researchers have found that a spinel ($Mg.Al_2O_4$) layer may form at or near the MgO surface under both static and dynamic flow conditions [Chen et al., 2005, Goto et al., 1997, Monaghan et al., 2004, Nightingale et al., 2005, Rait, 1997, Tran et al., 1998]. Evidence from quenched samples has suggested that the spinel forms at the liquid/solid interface, but then often becomes detached from the solid unless anchored by protrusions on the solid MgO surface. Therefore, this layer can be easily removed by forced liquid flow. Similar observations were made during studies of indirect dissolution of alumina-based materials in contact with a variety of slag types by Sandhage et al., 1988.

In situ observation of MgO dissolution, by Valdez et al., 2001, has confirmed the formation of spinel, but as the focus of the study was inclusion dissolution, the location of initial formation was not observed. A second study using high temperature microscopy by Nightingale et al,. 2004, designed to observe indirect dissolution of MgO refractory in $CaO-Al_2O_3-SiO_2$ slags found that spinel crystals formed quickly at the interface. However, significant liquid flow occurred during the experiment, and the spinel crystals broke away from the interface and were quickly carried out into the slag. Visibility of the crystals was obscured by the coarse grained, opaque nature of the refractory grade material limiting the information that could be extracted from these experiments.

Studies by Monaghan et al., 2005 and 2006 using confocal microscopy to monitor spinel inclusion dissolution in $CaO-SiO_2-Al_2O_3$ slags showed that though the mobility of the reacting species was fast and the inclusions were small (approximately 60 to 80 μm in diameter) the process was resolvable using standard video recording rates.

What is presented here is an investigation into the spinel crystal growth behaviour on a MgO single crystal in a $CaO-SiO_2-Al_2O_3$ slag system using high temperature microscopy.

METHODOLOGY

The growth of spinel on MgO in a 40% CaO, 40% SiO_2 and 20% Al_2O_3 slag was measured using high temperature microscopy. The slag was prepared by mixing and pre-melting appropriate mixtures of laboratory grade oxide powders in a platinum crucible at 1550°C, quenching the fused slag and then crushing the resultant glass. This process was repeated to obtain a homogenous slag. The slag composition was selected to allow spinel formation and to ensure that the slag was transparent to the imaging system.

Powdered slag was then packed into 5mm diameter Pt crucibles, melted at 1450°C, and then quenched. The slag was inspected using an optical microscope to ensure that it was free of crystalline material prior to the experiment.

Thin slices (1mm thick) of MgO were cut from single crystals, and the surface polished using diamond media to a 9μm finish. This slice was then divided into small pieces approximately 2x3mm. One piece

of MgO was then placed on top of the cold slag in the Pt crucible. The weights of the slag and MgO were recorded. The mass ratio of slag to MgO was approximately 7.

The prepared sample was then placed in an infra-red furnace attached to an optical microscope with a digital recording system. (see Figure 1) Samples were heated in air at 100^oC/min to 1420, 1440 or 1460^oC and then held at the desired temperature whilst crystal growth was observed. Images were recorded directly to a computer in digital format at 30 frames/s. At least two separate experiments were done at each hold temperature. The temperatures quoted have been corrected to account for the remote position of the thermocouple.
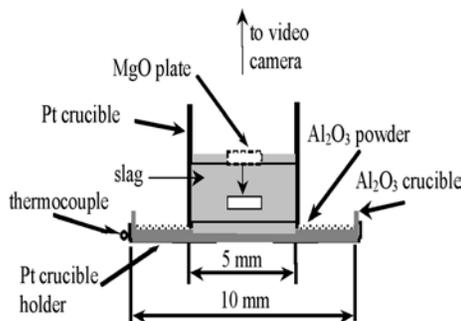

Figure 1: A Schematic showing the sample and crucible configuration and location of experimental thermocouple.

Video still images were extracted from the video recordings at approximately 10s intervals. Time zero was defined as the point that the crystals first became visible. The individual crystal size was determined by measuring the lengths of the sides of the base of the crystal, and the average calculated. Spatial measurements in both vertical and horizontal directions were calibrated using an E.Leitz Wetzlar graticule. Only crystals that were clearly in focus, and did not overlap with other crystals were measured. These measurements were then used to establish the spinel growth kinetics and are detailed and explained in the following sections.

RESULTS AND DISCUSSION

As the temperature increased and the slag started to melt the MgO substrate was observed to sink below the surface of the slag. The first crystals became visible within seconds of submersion. A typical sequence of digital still images captured from the video recordings of crystal growth is shown in Figure 2. In Figure 2 it can be seen that the crystals have a well-developed faceted morphology, displaying the octahedral form typical of a cubic crystal bounded by (111) planes. This morphology was observed in all experiments.

As the experiments progressed, some dissolution of the crystals was observed, and some crystals began to overlap. No further measurements of size were taken from crystals once either of these phenomena was observed. Results of the measurements of the size of the crystals as a function of time are shown in Figure 3 to 5 for temperatures 1420, 1440 and 1460°C respectively.

Thermodynamic calculations using MTDATA indicated that $MgAl_2O_4$ would be expected to form under the experimental conditions. MTDATA is a thermodynamic software package developed at the

National Physical Laboratory in the UK [Davies et al., 1994]. The morphology of the crystals observed in this study is consistent with the phases predicted by the thermodynamic calculations. Further, one sample from a similar experiment was quenched, sectioned and polished for examination in the SEM. EDS analysis of the crystals yielded a composition of 74% Al_2O_3 and 25.9% MgO, confirming that the crystals are spinel.
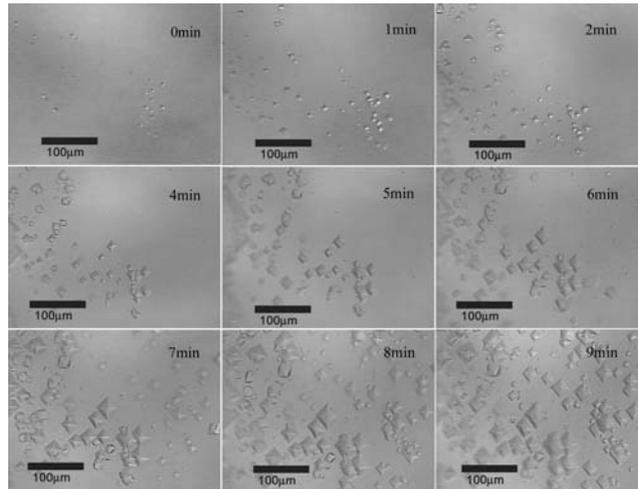

Figure 2: Video still image sequence showing spinel crystal growth at 1460°C.
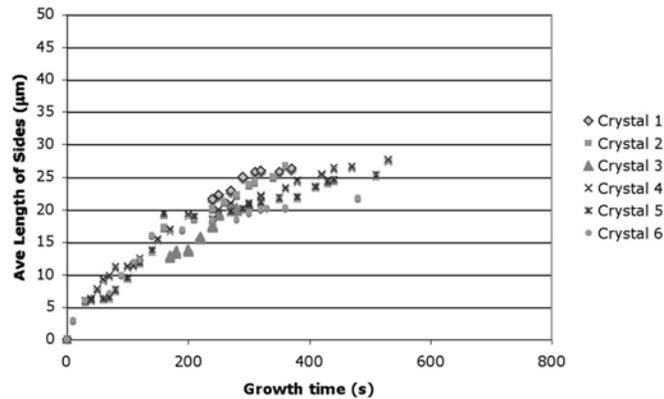

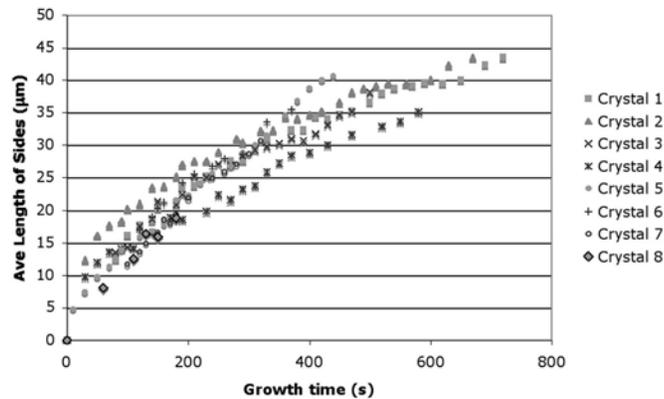Figure 3: Base length of pyramid versus time at 1420 °C.

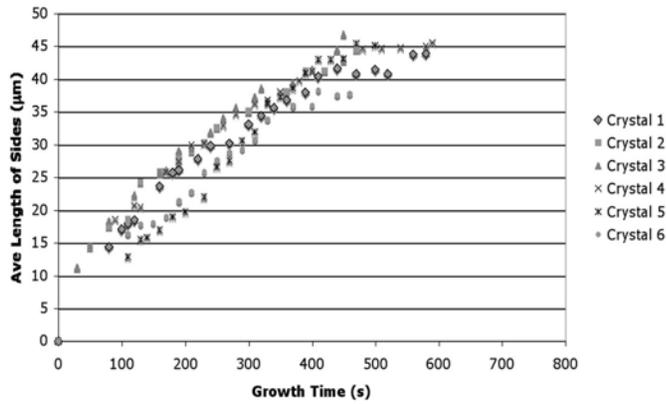Figure 4: Base length of pyramid versus time at 1440 °C (c) 1460°C.

Figure 5: Base length of pyramid versus time at 1460°C.

Layer growth kinetics are often well represented parabolic rate law [Poirier et al., 1994] given in equation (1)

$$\int_0^x x\,dx = \int_0^t k\,dt \qquad (1)$$

and (2)

$$x^2 = 2\,k\,t \qquad (2)$$

In this approach the kinetics of formation of a reaction product on a surface (layer) is commonly analysed by considering the counter-diffusion of cations through the layer. A schematic showing the growth of a $MgAl_2O_4$ spinel layer on MgO is given in Figure 6.
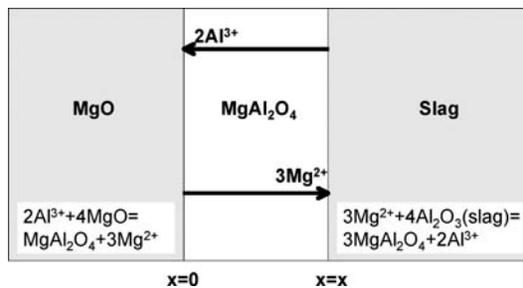

Figure 6: A schematic showing the growth of a spinel ($MgAl_2O_4$) layer on MgO.

This model is not directly applicable to these experiments as it considers the formation of a layer of uniform thickness, and not specifically the growth of pyramidal crystals. To facilitate its use the following approach has been adopted.

The base length (a) of the pyramid as measured in the experiments has been used to calculate the pyramid height and volume. As the spinel $MgAl_2O_4$ is an AB_2X_4 structure type where A and B

represent two different cations and X represents the anion [Callister, 2007], the height (h) and volume (V) can be calculated from equations (3) and (4).

$$h = \frac{a}{\sqrt{2}}$$ (3)

$$V = \frac{1}{3}a^2 h$$ (4)

From this volume (V) an effective layer thickness (x') was calculated using equation (5) assuming that this volume represented a cuboid with a square base of length a.

$$x' = \frac{V}{a^2}$$ (5)

The parabolic rate equation give in equation 2, was evaluated using the effective layer thickness x' calculated from the experimental spinel growth data and plotted in Figure 7. The solid line represents linear regressions of the data. Regression equations and their R^2 values are also given in the Figure. For a given temperature each data point represents an average of all experimental runs shown in Figures 3 to 5 at a given time.
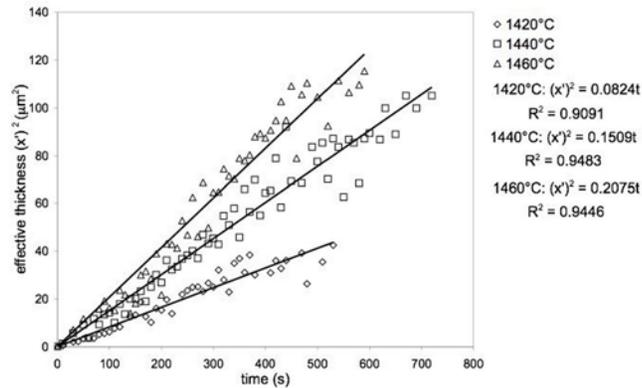

Figure 7: A plot of effective thickness versus time for all experiments.

From Figure 7 it can be seen that a plot of the square of the effective layer thickness versus time is linear and that increasing temperature increases the rate of growth of the layer. Further, the high R^2 value (>0.9) for the linear regression lines indicate that the lines are a good fit to the experimental data.

The linear relationship between x'^2 and time is consistent with what is expected from the parabolic rate expression given in equation (2) indicating that the growth of the spinel crystals is parabolic. An explanation of the effects of temperature on the spinel growth can be found by considering the effects of temperature on k. The k value in equation (2) has an Arrhenius relationship with temperature as shown in equation (7) [Poirier et al., 1994].

$$k = k_o e^{-E/(RT)}$$
(7)

From equation (7) it can be seen that increasing temperatures, increases k exponentially. This in turn results in an increase in the growth rate of the spinel. The Arrhenius relationship k has with temperature relates to the mobility of the diffusing ions in the spinel layer [Poirier et al., 1994]. The k_o constant and activation energy E from equation (7) were evaluated graphically from an Arrhenius plot (Figure 8) and found to be $2.15 \times 10^{16} \mu m^2 s^{-1}$ and 564 kJ mol^{-1} respectively.
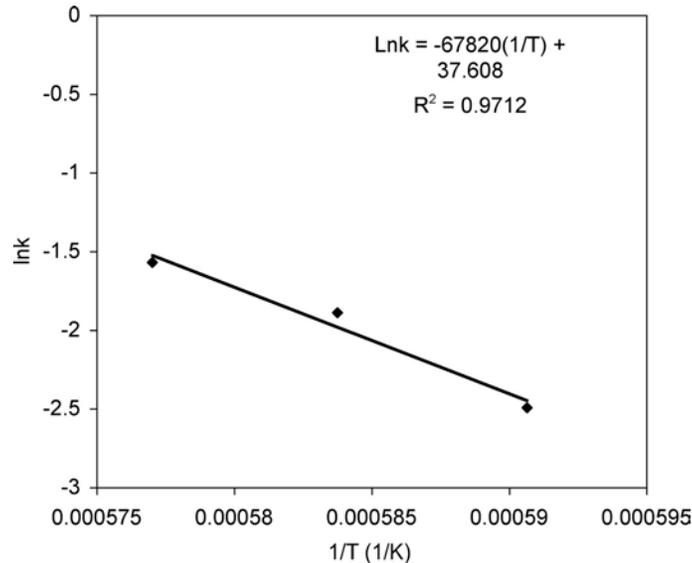
Figure 8: An Arrhenius plot of the parabolic rate constant k.

Given that these values have been obtained from a regression fit to three data points they should be considered as indicative only. Though these values can only be considered indicative the activation energy calculated for these experiments is comparable with a value of 401 kJ mol^{-1} for the Mg^{2+} diffusion coefficient in a spinel ($MgAl_2O_4$) obtained from high temperature (1200 to 1400°C) diffusion data reported in Kofstad, 1966, and 419 kJ mol^{-1} reported by Navais, 1961.

From this investigation little can be stated about the diffusing cations Mg^{2+} and Al^{3+}. The diffusion coefficient of these ions is inversely proportional to their ionic radii [Poirier et al., 1994]. Therefore given their respective ionic radii are 0.072 and 0.053 nm [Callister, 2007], it would be expected that the larger Mg^{2+} ion would have a lower mobility in the spinel layer. Though not indicated in Figure 5, there is the possibility of O^{2-} migration. However, given its large size, 0.140 nm [Callister, 2007], relative to Mg^{2+} and Al^{3+}, this is considered unlikely.

After a period of growth on the MgO substrate many crystals were observed to detach from the substrate, and move into the bulk of the slag. This has been explained by considering the volume change associated with the phase transformation from MgO to $MgAl_2O_4$. The lattice parameter of the spinel (0.808 nm) [Ball et al., 2005] is almost double that of MgO (0.421 nm) [McClune, 1984], resulting in significant mismatch and strain at the interface which could lead to fracture and detachment of the spinel crystals. This detachment is consistent with what has been previously

reported by the authors on the kinetics of dissolution of polycrystalline MgO. [Nightingale et al., 2005].

CONCLUSIONS

The growth kinetics of $MgAl_2O_4$ spinel on single crystal MgO in a 40% CaO-40% SiO_2-20% Al_2O_3 slag, as measured by high temperature microscopy, are consistent with the parabolic rate law. Further, detachment of the spinel crystals observed late on in the experiments have been explained by the large difference in lattice parameters between MgO and $MgAl_2O_4$, resulting in strain and consequently fracture at the interface. A provisional activation energy of 564 kJ mol^{-1} has been obtained for the crystal growth process. This value is consistent with other data reported in the literature for comparable conditions.

NOMENCLATURE

x	spinel ($MgAl_2O_4$) layer thickness in $\square$m
x'	spinel ($MgAl_2O_4$) layer effective thickness in $\square$m
k	parabolic rate constant in $\mu m^2 s^{-1}$
t	time in seconds.
a	base length of pyramid as measured in the experiments in μm
h	pyramid height in μm
V	pyramid volume in μm^3
k_0	Arrhenius constant in $\mu m^2 s^{-1}$
E	activation energy, kJ mol^{-1}
R	gas constant 8.314 $JK^{-1}mol^{-1}$
T	temperature in C$^\circ$ or K

ACKNOWLEDGEMENTS

REFERENCES

Ball J.A., M. Pirzada, R.W. Grimes, M.O. Zacate, D.W. Price and B.P. Uberuaga, (2005) Journal of Physics: Condensed Matter, 2005, 17, pp. 7621-7631.

Callister W.D. (2007). Materials Science and Engineering an Introduction (7 ed); New York, USA, John Wiley and Sons Inc., pp. 418-424.

Chen Y., G.A. Brooks and S.A. Nightingale (2005). Canadian Metallurgical Quarterly, 44 (3), pp. 323-329.

Davies R.H., A.T. Dinsdale, J.A. Gisby, S.M. Hodson and R.G.J. Ball (1994). Conference On Applications Thermodynamics on the Synthesis and Processing of Materials, ASM/TMS, Rosemont, IL, USA, p.371.

Goto K., B.B. Argent and W.E. Lee (1997). J. Am. Ceram. Soc., 80 [2], pp. 461-7.

Kofstad P. (1966). High Temperature Oxidation of Metals; 1966, New York, USA, John Wiley and Sons Inc., pp. 306-308.

McClune W.F. (1984) International Diffraction File, Inorganic Volume, JCPDS International Center for Diffraction Data, Vol. 4, p. 832.

Monaghan B.J., S.A. Nightingale, L. Chen and G.A. Brooks (2004). Proc of VII Inter. Conference on Molten Slags Fluxes and Salts Cape Town, South Africa, 25 – 28 January, pp. 598-607.

Monaghan, B.J., L. Chen and J. Sorbe (2005). Ironmaking and Steelmaking, Vol 32, pp258-264.

Monaghan, B.J. and L. Chen (2006). Ironmaking and Steelmaking, Vol. 33, pp323-330.

Navais L. (1961). J of the American Ceramic Society, 44 (9), pp. 434-446.

Nightingale S.A. and B.J. Monaghan (2004). Proc. of Austceram & 3rd Inter. Conference on Advanced Materials Processing, Nov 30-Dec, Melbourne, pp.130-131.

Nightingale S.A., G. A. Brooks, and B.J. Monaghan (2005). Metallurgical and Materials Transactions B, Vol 36B, Iss. 4, pp. 453-461.

Poirier D.R. and G.H. Geiger (1994). Transport Phenomena in Materials Processing, Warrendale, PA, USA, TMS, pp. 444-493.

Rait R. (1997). PhD thesis, University of Melbourne, Australia, 1997.

Sandhage K.H. and G.J. Yurek (1988). J. Am. Ceram. Soc., 71 [6], pp. 478-89.

Tran T., S. Nightingale and G. Brooks (1998). J. Aust. Ceram. Soc., 34, pp. 33-38.

Valdez M., K. Prapakorn, A.W. Cramb and S. Sridhar (2001). Steel Research, 72, pp. 291-297.